Chemistry–A European Journal
Research Article
doi.org/10.1002/chem.202201081
Chemistry Europe
European Chemical Societies Publishing
www.chemeurj.org

Phosphorescence Induction by Host-Guest Complexation with Cyclodextrins – The Role of Regioisomerism and Affinity

Matthias Hayduk,[a] Torsten Schaller,[a] Felix C. Niemeyer,[a] Kevin Rudolph,[a] Guido H. Clever,[b] Fabio Rizzo,*[c, d] and Jens Voskuhl*[a]

Abstract: We present an in-depth investigation of cyclodextrin complexes with guest compounds featuring complexation-induced room temperature phosphorescence (RTP) in aqueous solution. Very interestingly, only the complexed regioisomers bearing lateral substituents on meta-position show RTP, whereas the stronger host-guest systems with para-substituted dyes show no RTP features. The reported systems were investigated regarding their complexation behavior in water using isothermal titration calorimetry and mass spectrometry. In the case of γ-CD very strong 1:1 inclusion complexes (K_a up to 5.13×10^5 M^{-1}) were unexpectedly observed. It was found that not only a strong binding to the cyclodextrin cavity is needed to restrict motion, inducing the emission, but also the conformation inside the cavity plays a pivotal role – as supported by an extensive NMR study and MD simulations.

Introduction

The investigation of novel materials showing room temperature phosphorescence (RTP) properties is an outstanding field of research due to its potential use in various optical applications spanning from devices, such as OLED's[1] and solar cells, to bioimaging.[2] Although many examples of metal complexes have been reported in literature,[3] metal-free aromatic materials are attracting growing interest due to their chemical versatility.[4] Commonly used strategies for achieving pure organic RTP emission focus on the enhancement of the intersystem crossing (ISC) process and restriction of non-radiative decay.[5] To satisfy these requirements, pure organic RTP emission in the solid phase can be achieved via immobilization in a polymer matrix,[6] crystallization,[7] halogen bonding,[8] self-assembly,[7c] and H-aggregation.[9] However, the most challenging feature is the achievement of systems able to generate RTP in solution, especially in aqueous phase. Indeed, the free rotational motion and the high concentration of oxygen in water lead to the quenching of RTP as consequence of the favourite nonradiative decay processes versus phosphorescence.

Supramolecular assembly appears as valuable approach to overcome the abovementioned limitations in aqueous phase. In particular, host-guest interactions between cyclic molecules and organic dyes allowed to develop pure organic RTP systems.[10] Commonly used host compounds are cucurbiturils (CB) and cyclodextrins (CD). CBs are cylindrical structures able to host up to two molecules, which show specific properties upon their mutual interaction inside the cavity. Very recently, Ma et al. used this approach to obtain RTP in aqueous solution for the first time.[11] However, the emission arises from the interaction of the two dyes, thus difficult to predict due to the mutual interactions host-guests and guest-guest.[12] The possibility to obtain metal-free RTP emission in water by means of a single emitting molecule thus remains a challenging feature. CDs as a well known class of cyclic host molecules in the field of supramolecular chemistry and have been studied for decades by numerous groups around the world.[13] Their special structure, featuring a hydrophobic cavity able to encapsulate guest compounds, their low price as well as their facile modification, make them ideal candidates for the investigation of supramolecular encapsulation[14] and can they be viewed as small artificial minimized protein pocket.[14c,15] The supramolecular host-guest ability of CDs has been used to

[a] M. Hayduk, Dr. T. Schaller, Dr. F. C. Niemeyer, K. Rudolph, Prof. Dr. J. Voskuhl
Faculty of Chemistry (Organic Chemistry), ZMB and CENIDE
University of Duisburg-Essen
Universitätsstraße 7, Essen 45141 (Germany)
E-mail: jens.voskuhl@uni-due.de

[b] Prof. Dr. G. H. Clever
Technische Universität Dortmund
Fakultät für Chemie und Chemische Biologie
Otto-Hahn-Straße 6, 44227 Dortmund (Germany)

[c] Dr. F. Rizzo
Institute of Chemical Science and Technologies "G. Natta" (SCITEC)
National Research Council (CNR)
via G. Fantoli 16/15, 20138 Milano (Italy)
E-mail: fabio.rizzo@cnr.it

[d] Dr. F. Rizzo
Center for Soft Nanoscience (SoN)
Westfälische Wilhelms-Universität Münster
Busso-Peus-Str. 10, 48149 Münster (Germany)

Supporting information for this article is available on the WWW under https://doi.org/10.1002/chem.202201081

tune the emission properties of different classes of dyes in a 1:1 ratio. In particular, CDs have been employed to control the emissive properties in aqueous solution of compounds showing aggregation-induced emission (AIE), which has attracted interest in the field of supramolecular chemistry.[16] The reason of this growing scientific attention arises from the emission of these typically propeller shaped compounds, which cannot only be induced by aggregation or in the solid state, but also when entrapped in a sterically hindered environment, such as a protein pocket or a supramolecular host.[17] In these particular surroundings, the phenomenon of restriction of intramolecular motion (RIM) comes into play.[18] The free motion in solution leads to a conversion of absorbed light mainly into motion or heat, whereas hindered motion opens radiative decay pathways from the excited state. First attempts to induce emission by supramolecular entrapment were conducted by synthesizing a water-soluble tetraphenylethene (TPE) derivative bearing boronic acids to be complexed with carbohydrates (in this case β-cyclodextrins), or encapsulation via hydrophobic interactions.[19] It was found that a cooperative binding occurs by means of different binding modi. Later, Zheng and coworkers showed the first stable 1:1 emissive complex between a TPE derivative with γ-cyclodextrin. Here a shift between aggregate emission (λ_{em} = 485 nm) and a dissolution of the aggregates by CD-complexation (λ_{em} = 388 nm) was observed.[20] In 2016 Bai and coworkers showed that the complexation of the whole AIE luminophores is not necesssary to induce a fluoresecence emission. By using a mono-phenylcarboxyl-decorated TPE able to form a complex with α-CD, they showed a reversible "increasing-decreasing" emission by introducing a photoresponsive competitive binding molecule based on azobenzenes.[21] Another reported example involves the interaction of two pyrene units inside γ-CDs leading to excimer formation, which can be followed by the bathochromic shift in fluorescence emission.[22]

To summarize, some examples of complexation induced emission by means of CDs have been reported, but are limited to fluorescent systems On the contrary, only few examples of supramolecular systems for RTP based on host-guest interactions have been shown, mainly based on the combination of β-CDs and napthalene.[23]

Moreover, to the best of our knowledge, there are no related studies on other types of CDs used for RTP materials, especially on γ-CD (eight glucose subunits). In this context, the investigation of novel supramolecular host-guest systems as RTP materials appears very innovative.

Among dyes showing RTP properties, the persulfurated benzene-based molecules attract a rising interest due to high spin-orbit coupling arising from the heavy sulphur atoms. In particular, compounds based on tetra-mercaptophenol have been recently investigated as AIE luminogens with long-lived emission.[24] However, the reported studies are carried out in organic solvents or in mixture water/organic solvent, which hampers the possibility to perform investigation on isolated dyes in aqueous solution.

Aiming to add an important step on the palette of RTP dyes in aqueous solution, in this contribution we report the synthesis of the water-soluble tetra-mercaptophenol based dyes and their supramolecular host-guest interactions with different classes of CDs. In particular, we describe for the first time room temperature phosphorescence generated in water by the formation of highly stable 1:1 complexes between tetra-sulfonated or carboxylated guests and γ-cyclodextrin based on a restriction of intramolecular motion (Figure 1).

Results and Discussion

The synthesis of the four target compounds was carried out by synthesizing first the tetra-mercaptophenols, using either 3- or 4-mercaptophenol under basic conditions according to a previously described modified procedure.[24–25] The sulfonates PTS (para-tetra-sulfonate) and MTS (meta-tetra-sulfonate) were obtained by reaction of the desired tetramer with propanesultone in the presence of base,[26] whereas the carboxylates PTC (para-tetra-carboxylate) and MTC (meta-tetra-carboxylate) were obtained by substitution with *tert*-butyl-bromoacetate followed by subsequent acidic and basic deprotonation.[27] All compounds were purified by medium pressure liquid chromatography (MPLC) yielding the compounds as potassium salts with an appearance colour from yellow to red. The compounds revealed high water solubility without the appearance of noteworthy emission (see below, Figure 5). This behaviour could be attributed to a free rotational and vibrational motion arising from the full solvation, and hence to the conversion of absorbed energy into motion. This feature is characteristic for AIE emitters and has been described numerous times beforehand.[28] Additionally, we were interested on the effect of the complexation with different cyclodextrins in aqueous media, by using α- (six glucose units), β- (seven glucose units) and γ-cyclodextrin (eight glucose units). Thus, we performed photophysical characterisation of the pure compounds in presence and absence of cyclodextrins in 1:1 ratio.

Complexation behaviour

To ensure the formation of stable host-guest complexes, isothermal titration calorimetry (ITC) was performed for all

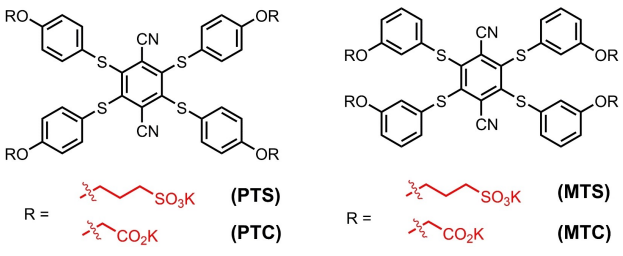

Figure 1. Molecular Structures of the guest luminophores for the complexation with cyclodextrins.

possible combinations of the four guest compounds and the three cyclodextrins (α-, β-, γ-CD) of interest (Figure 2 and Figures S23–25 in Supporting Information).

Remarkably, MTS and MTC bind to γ-CD in a 1:1 fashion with an unexpected high association constant (up to 1.53×10^5 M^{-1} for MTS). It is worth noting that these high values are quite unusual for this class of cyclodextrins and comparable values have been reported only for nanodiamonds[29] and borate clusters.[30] Even more interestingly, PTC and PTS showed binding towards γ-CD with outstanding association constants (up to 5.13×10^5 M^{-1}), indicating the favourable size of the designed derivatives to act as guest for γ-cyclodextrin (Table 1 and Table S3). It is important to emphasize that the association constant values here reported for all four compounds are among the highest constants for host-guest complexes between γ-CD and pure organic molecules, to the best of our knowledge.

On the contrary, the four compounds bind to β-CD, showed only weak to moderate association constants (Figure S24 and Table S3) and no interaction with α-CD (Figure S25), which fits well to our hypothesis that the smaller cavities are unable to fully encapsulate the guest compounds. The weak, but detectable binding of the guests with β-CD can be attributed to a partial encapsulation of the phenyl rotors, which was also observable in mass spectrometry (Figures S30–33).

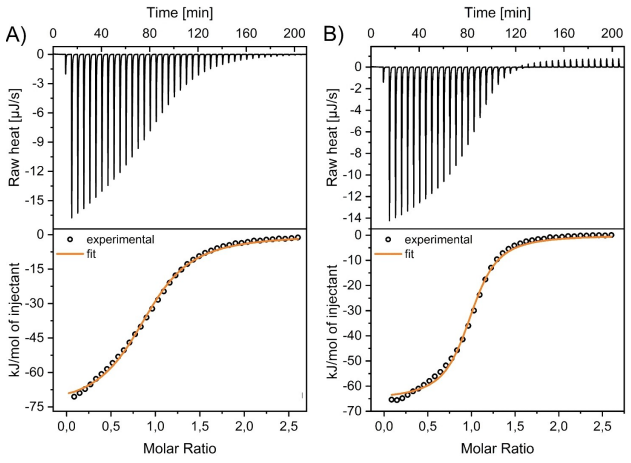

Figure 2. A) ITC titration of MTS with γ-CD B) ITC titration of PTS with γ-CD. Upper graph: raw heat signals, lower graph: integrated heat peaks and the corresponding fit. Fitting was performed using a 1:1 model. [guest] = 1 mM, [host] = 0.08 mM, T = 293 K.

Table 1. Complex formation thermodynamics as obtained by ITC measurements with γ-cyclodextrin. ITC was performed in the normal titration mode by titrating 1 mM guest to 80 µM host, T = 293 K. Titration were performed as duplicates. For mean deviations see Supporting Information.

	N	K [M^{-1}]	ΔH [kJ/mol]	ΔS [J/K*mol]	ΔG [kJ/mol]
PTS	0.93	4.99×10^5	−63.07	−102.3	−32.94
MTS	0.90	1.53×10^5	−73.20	−146.23	−30.01
PTC	1.07	5.13×10^5	−52.72	−67.37	−32.80
MTC	1.13	1.52×10^5	−48.12	−62.34	−29.67

To classify our newly designed complexes into the family of γ-CD host-guest systems, we plotted the entropy versus the enthalpy to investigate the entropy-enthalpy compensation (Figure 3). By comparing with classic guests for γ-CD,[31] such as azobenzenes, aromatic compounds, and cage-like hydrocarbons, it is obvious that our highly flexible compounds populate another area in this plot, revealing drastically enhanced enthalpy values compensated by an increased entropic contribution. Typically, complexes with γ-CD are considered as weak, due to the highly flexible nature of the γ-CD (8 glucose units) compared to the more rigid appearance of β-CD (7 glucose units). This behaviour can be attributed to two phenomena: 1) the cavity of β-CD is more rigid and thus reveals a higher hydrophobicity due to a closed intramolecular hydrogen bonding network, and 2) γ-CD lacks of high energy water (due to the flexibility) typically enhancing the affinity to smaller hosts. In 2015 Nau et al. described the highest association constant ever determined for a γ-CD inclusion complex.[30a]

Inorganic borate cluster, such as $[B_{12}Br_{12}]^{2-}$, were found to bind to γ-CD with association constants of up to one million going along with high enthalpies and a significant entropy compensation (see the blue spots in Figure 3). The rigid spherical shape of these inorganic compounds as well as their high polarizabilities were identified to be the reason for these high affinity constants. Furthermore, it was expected that the host wraps around the $[B_{12}Br_{12}]^{2-}$ optimizing the dispersive interactions.[30a] Our system combines a highly flexible host and a guest with four phenyl-rotors exhibiting free motion in aqueous media. As consequence, two flexible compounds were expected to mutually adapt leading to an optimal fitting (by optimisation of dispersive interactions) inside the cavity. We believe that the chaotropic effect previously described by Nau et al.[30] can be also applied to our compounds. This means that our hydrophilic compounds are able to break

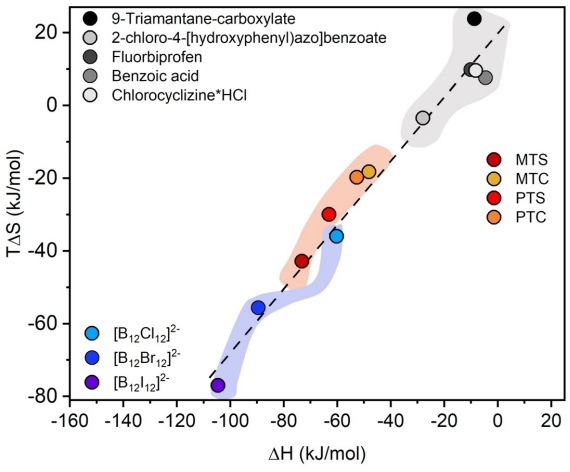

Figure 3. Comparison of the enthalpy-entropy compensation for selected literature known examples of γ-CD complexes with the complexes investigated in this study using MTC, MTS, PTC and PTS as guests for γ-CD (data taken from Refs [29a, 30a, 31]). Coloured clouds are used to guide the eye and to identify compound classes.

hydrogen bonds in their surrounding water environment, followed by recovery of the water structure upon complexation with γ-CD, which results in negative entropic values characteristic of this effect.

The existence of 1:1 complexes of PTS, PTC, MTS and MTC with γ-CD was also confirmed by high resolution ESI-MS showing the molecular peaks for the corresponding complexes (Figure 4 and Figures S27–29). As example, Figure 4 shows the corresponding mass spectrum (negative ion mode) of MTS with γ-CD, revealing the existence of the molecular ion peak $[M]^{4-}$ of the inclusion complex with a molecular mass of 601.1091 g/mol, which is in excellent agreement with the calculated value of 601.1098 g/mol. A similar behaviour was observed for PTS, PTC and MTC revealing in all cases the presence of the 1:1 complexes (Figure. S27–29).

Besides 1:1 complexes, we also observed the potential formation of 1:2, 1:3 and 1:4 complexes with β-CD in mass spectrometry, although these results should be regarded as qualitative evidence (due to low resolved peaks, Figure S30–33). This finding is in good agreement with ITC measurements, showing a drastic deviation from $N \sim 1$ ($N < 1$, Table S3), which suggests stepwise encapsulation of single phenyl rotors in the β-CD cavity. This partial complexation, unable to restrict the motion of the corresponding luminophores efficiently, explains the absence of variations in the photophysical properties (see below).

Photophysical investigation

The four compounds show very similar absorption spectra, indicating that the position and the nature of the lateral chains are only slightly affecting the conjugation of the aromatic system. The major difference between the two families of molecules is the little bathochromic shift occurring at the lower energy band in PTS and PTC compared to the analogous *meta*-substituted dyes (MTS and MTC). Upon complexation with α- and β-CDs, the UV-Vis spectra are identical compared to the dyes alone (Figure S17 and S18), which can suggest the lack of (or limited) complexation. In case of γ-CD, the absorption bands are slightly modified for all compounds (Figure S16), indicating the occurrence of interaction between them.

The analysis of the emission reveals the most interesting difference between the two classes of dyes. The *para*-substituted PTS and PTC show negligible emissive properties alone in solution as well as in presence of α-, β- or γ-CDs (Figure 5A and 5B). In contrast, MTS and MTC show a completely different photophysical behaviour. In absence of cyclodextrins, the *meta*-substituted compounds exhibit a weak emission band with maximum at 440 nm and 470 nm for MTS and MTC, respectively (Figure S19 and S20). The fast lifetime decay (τ_{av} around 1 ns for both compounds, Table S1 and Figure S21) suggests the fluorescence as radiative mechanism.

Upon complexation, remarkable variation on the emission of MTS and MTC were observed. The presence of α- or β-cyclodextrin induces only marginal changes in the emission properties compared to the free dye, without a significant increase in intensity. Unexpectedly, γ-cyclodextrin provokes a dramatic change with the appearance of an intense emission band with maximum at 620 nm in both MTS and MTC, which is visible also by naked eyes under standard UV lamp (Figure 5C). The long mono-exponential lifetime values recorded in both compounds (1.22 and 1.79 μs for MTS and MTC, respectively, Figure S21 and Table S1 and S2) suggest

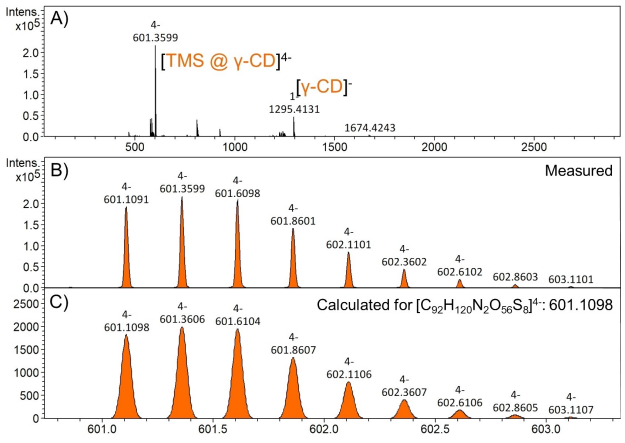

Figure 4. A) Overview HR-ESI-MS spectrum of MTS complexed by γ-CD, B) Isotopic pattern of the measured peak at 601.3599 g/mol, C) Calculated isotope pattern of MTS complexed with γ-CD.

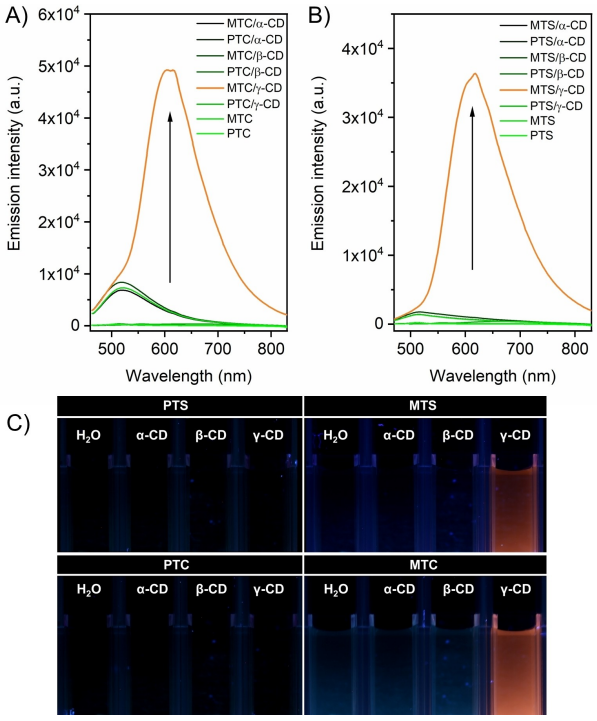

Figure 5. A) Emission spectra of MTC and PTC in the presence of 1 equivalent of different cyclodextrins. B) Emission spectra of MTS and PTS in the presence of 1 equivalent of different cyclodextrins, C) Photographs of the tetravalent anionic compounds used in this study, in the presence of one equivalent of different cyclodextrins under UV-light irradiation ($\lambda_{ex} = 365$ nm). [host] = [guest] = 100 μM in water.

the phosphorescent character of the orange emission and indicates the presence of one single species, namely the 1:1 inclusion complex. The assumption about the nature of the lower energy emission is further supported by the emission measurements performed under argon, showing an enhancement of intensity under anaerobic condition (Figure S22). The increased intensity observed at 620 nm after the removal of oxygen from solution indicates that the radiative decay occurs from the triplet state. This is in agreement with the photophysical behaviour of other mercaptophenyl derivatives reported in literature as RTP dyes.[24b,32] However, the literature data refer generally to dyes showing phosphorescence upon aggregation or embedded in rigid matrices. In contrast, the phosphorescence observed in our systems originates from the formation of an inclusion complex, which induces a restriction of the intramolecular motion (RIM) phenomenon. Besides that, it is also possible that the CD decreases the rate of oxygen quenching due to shielding, similar to the observed behaviour of pyrene upon encapsulation in cavitands.[33] However, in contrast with the pyrene, the quenching in our system is less efficient as suggested by the relative slightly increased emission under argon, which could be probably associated with the large size of the guests compared to size of the cavity. It is worth noting that the emission spectra exhibit a residual fluorescent band at higher energy (Figure S19 and S20), which could be attributed to the presence of free dye in solution. Indeed, this high energy emission band is not affected by the presence of oxygen (see Figure S22). This is consistent with the dynamic nature of the host-guest interaction of cyclodextrins.[34]

Additionally, we carried out fluorescence titration experiments by monitoring the emission band at 620 nm in relationship with the enhancing concentration of the host to further support the complexation between γ-CD and MTC and MTS. The fitting of the data leads to association constants comparable with the values obtained by ITC (Table 1) and the expected complexation stoichiometry ($N = 1{,}25$, $K_a = 1.6 \times 10^5\ M^{-1}$ for MTC and $N = 1.16$, $K_a = 3.83 \times 10^5\ M^{-1}$ for MTS) (Figure S56).

Although we were able to proof the existence of inclusion complexes with high association constants of all four guests with γ-CD, the different behaviour of the *meta*- and *para*-substituted tetramers in regard to their dissimilar emission behaviour needs further analyses, since a simple complexation and strong association seems not to be the only parameter affecting the emission properties. It is worth to note that this effect has not been observed before, or has been overseen, making the understanding of change on the emission behaviour pivotal.

To gain a deeper understanding, and since growing of single crystals failed, we decided to use advanced NMR techniques and molecular modelling to shine more light on the complexation and the influence of conformation of the guest compounds inside the CD cavity.

NMR measurements and molecular dynamics simulations

Despite some attempts, single crystals of the four complexes are not available; therefore, other methods for structural insights needed to be applied. Here, NMR is the obvious choice as numerous studies on cyclodextrin complexes have shown.[35]

As a first step, we performed ^{1}H NMR titrations with varying host/guest ratio as exemplary shown in Figure 6 for the PTS/γ-CD complex (Figure S34a–c). The ^{1}H resonances of PTS are well resolved from those of the γ-CD allowing the separate observation of intensities and shifts in the course of the titration. Having the high association constants determined by ITC measurements in mind, we were not surprised to see two signal sets for the guest molecules corresponding to the complexed PTS and to the non-complexed molecules, respectively. While their relative intensities follow the stoichiometry within the error limits, the chemical shifts characterizing the two states remain constant indicating the lack of exchange on the NMR time scale. In equimolar solutions, we expect to observe solely complexed molecules as illustrated in Figure 7 Obviously, the complexation leads to a loss of symmetry and, in consequence, to a doubling of the respective ^{1}H resonances. Two arrangements appear to be

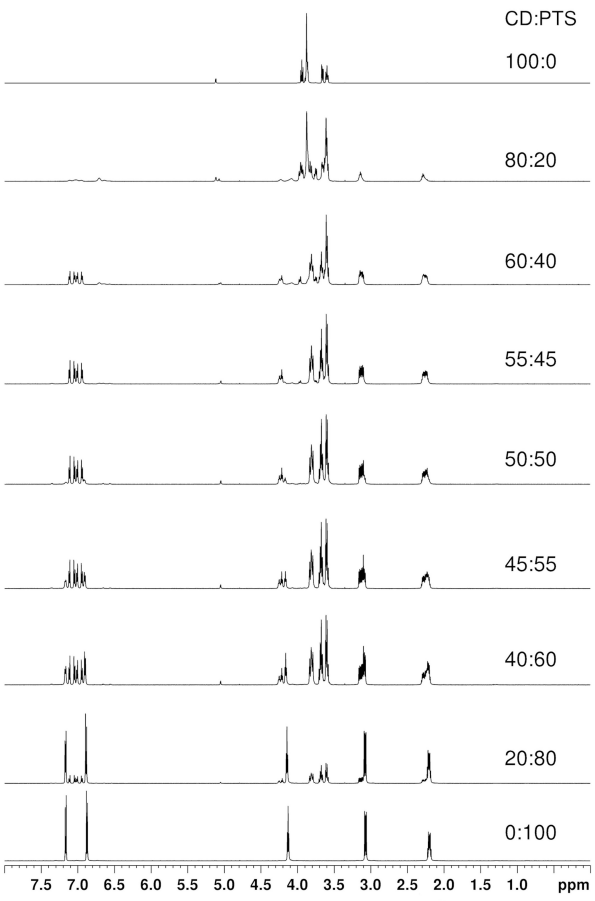

Figure 6. ^{1}H NMR titration for aqueous solutions of γ-CD complexes with PTS as guest.

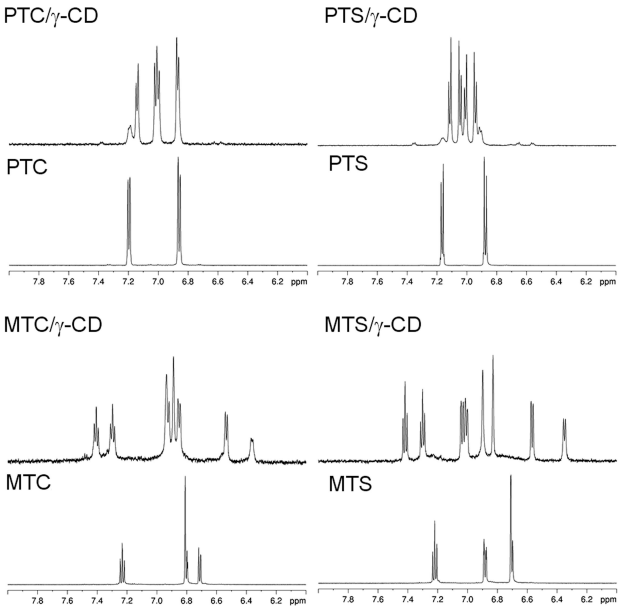

Figure 7. ^{1}H NMR spectra (aromatic region) of the free guest molecules and their 1:1 complexes with γ-CD.

possible: (A) the central phenyl ring of the guest molecule is centred inside the cyclodextrin cavity with the substituents pointing to the primary and secondary rim or (B) one part of the guest molecules is located within the cavity while the other part remains more or less outside. In both cases, the observation of two signal sets indicates either a static symmetrical arrangement or – more likely – to a fast rearrangement around this equilibrium state. Moreover, it is clear that the complexation appears in a symmetry-conserving way, that is, we can rule out that only one of the four phenylcarboxylate/phenylsulfonate moieties is located inside the cyclodextrin cavity.

Comparing the ^{1}H resonances of the free guest molecule with those of the complexed ones, we noticed shifts of the signals high – and downfield as well, thus ^{1}H COSY experiments (Figure S34d) were performed to assign the now different aromatic rings. The data are summarized in Table 2.

In most NMR studies on cyclodextrin complexes, the ^{1}H chemical shift of the CD protons are detected and used as a proof for complexation and as key for structural interpretations.[29b,35] At lower complexation constants, a continuous shift of these signals is observed, and the maximal shift is either found experimentally or determined by fitting the respective titration curves. In our case, such an approach did not work: starting with a 40:60 ratio of guest and CD, the positions of the – at least partially – overlapping resonances remain almost constant making it impossible to follow the ^{1}H shifts of CD and to determine the maximum shift on the conventional way. However, the ^{1}H NMR shift of the CD protons depends on the guest molecule (see Figure S38) resulting in specific spectral patterns due to differing complex structures.

Therefore, we performed a ^{1}H–^{13}C HSQC experiment at each titration step in order to retrieve the ^{1}H and, in addition, the ^{13}C chemical shifts of all cyclodextrin complexes thanks to the improved resolution. In Figure 8, an overlay of two such spectra for PTS is shown as example.

As expected, we observe shifts of the cyclodextrin signals to lower frequencies up to 0.3 ppm in the ^{1}H dimension, while the ^{13}C chemical shifts were significantly less affected. The common interpretation of this finding is that the proximity of the cyclodextrin protons to the aromatic parts of the guest molecules results in a stronger shielding and leads to the respective chemical shift changes. Obviously, the six protons are influenced to a different degree by this effect. The most prominent shift occurs for H3 and, somewhat surprisingly, for one of the H6 methylene protons (denoted with H6b). More remarkably, this effect appears independent from the nature of the four guest molecules of this study, as summarized in Table 3.

In other words, the changes of chemical shift alone do not provide sufficient information to distinguish possible differences in the geometry of the complexes. We therefore used ^{1}H NOESY and ROESY experiments to extract information about the spatial relations between the guest molecules and the

Table 2. ^{1}H chemical shifts of the guest protons after complexation with γ-CD. The chemical shifts of the free guest molecules are summarized in the Supporting Information. Ring 1 denotes the two phenyl rings of the phenylcarboxylate/phenylsulfonate moiety inside the CD cavity, ring 2 the rings outside.

	PTC	PTS	MTC	MTS
ring 1 (inside) ^{1}H shifts (ppm)	7.13 (d) 7.00 (d)	6.94 (d) 7.01 (d)	7.30 (t) 6.93 (s) 6.85 (d) 6.36 (d)	7.30 (t) 7.01 (d) 6.91 (s) 6.35 (d)
ring 2 (outside) ^{1}H shifts (ppm)	6.99 (d) 6.86 (d)	7.04 (d) 7.11 (d)	7.41 (t) 6.93 (d) 6.88 (s) 6.53 (d)	7.42 (t) 7.04 (d) 6.83 (s) 6.57 (d)

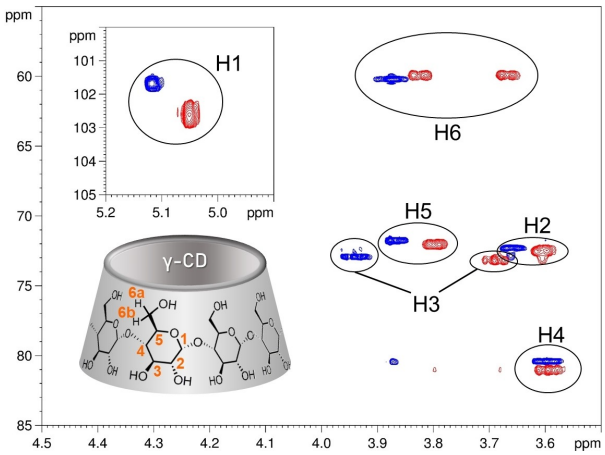

Figure 8. ^{1}H–^{13}C HSQC NMR spectra of γ-cyclodextrin (blue) and its 1:1 complex with PTS (red). Note the different shifts of the CD signals after complexation and the splitting of the H6 resonance into two separate signals H6a (3.83 ppm) and H6b (3.67 ppm).

Table 3. Maximum ^{1}H chemical shift change (in ppm) of the γ-cyclodextrin protons after complexation with γ-CD.

	H1	H2	H3	H4	H5	H6a	H6b
CD [ppm]	5.117	3.660	3.942	3.597	3.872	3.874	3.874
PTC/γ-CD	−0.082	−0.112	−0.302	−0.022	−0.110	−0.066	−0.237
MTC/γ-CD	−0.084	−0.106	−0.243	−0.024	−0.083	−0.063	−0.237
PTS/γ-CD	−0.066	−0.053	−0.259	−0.003	−0.067	−0.049	−0.207
MTS/γ-CD	−0.094	−0.075	−0.305	−0.028	−0.118	−0.074	−0.250

cyclodextrin. The nuclear Overhauser effect – strongly dependent on the dipolar interaction between protons in close proximity – should result in significant cross peaks in the respective two-dimensional spectra or to measurable intensity changes in the one-dimensional version of such experiments.

These experiments have been carried out on equimolar solutions (CD:guest = 50:50) with different mixing times ranging from 50 to 400 ms. Figure 9 reports a ROESY spectrum of the PTS-cyclodextrin complex. As expected, we observe off-diagonal peaks as a sign of dipolar interaction within the cyclodextrin and the sulfonate moiety of the guest. More interestingly, we detect a number of cross-peaks between the phenyl ring signals of the guest molecule and the CD – resonances as shown in Figure S34g. Noteworthy, the intensities and the position of the cross peaks differ from one guest proton to the other. This means that interpreting this result as a measure of the dipolar interactions and thus as a measure of the distances between the protons within the complex is a useful tool for better understanding the structure of the complexes.

By analysing Figure 9 in detail (see Figure S34g), we see that the guest resonances assigned to ring 2 show a much smaller Overhauser effect as those of ring 1, in particular to the protons H3 and H5 (3.68 and 3.80 ppm, respectively) inside the CD cavity. This finding rather supports arrangement B (discussed above) where ring 2 is located outside the cavity whereas ring 1 is the moiety inside the cyclodextrin establishing close ^{1}H–^{1}H contacts. Furthermore, one proton each from ring 1 and ring 2 is in close proximity to a methylene group of the sulfonate unit, which allows the assignment of the complexation-shifted signals to the specific hydrogens on the aromatic ring of the guest.

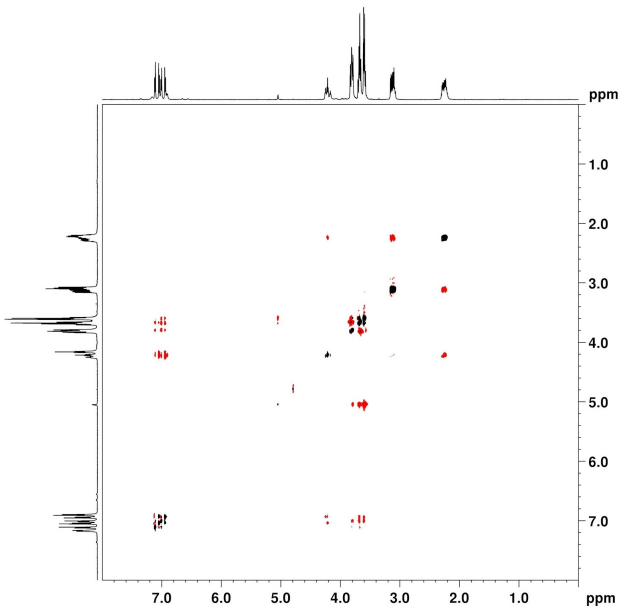

Figure 9. ^{1}H ROESY spectrum for a equimolar aqueous solution of γ-CD with PTS.

Remarkably, we find additional correlations within the signals of the guest molecule (shown in Figure S34 h). Beside the expected negative cross-peaks due to dipolar interactions within one ring, we observe positive correlation peaks between resonances of ring 1 and 2. Moreover, these correlations are detected between protons assigned to the same position on the phenyl ring: we find cross-peaks at 7.11/7.01 ppm as well as at 7.01/6.94 ppm. In ROESY experiments, correlation peaks due to the nuclear Overhauser effect always appear with reversed phase compared to the diagonal signals – the cross peaks observed here point to an exchange phenomenon. On the timescale of the ROESY mixing time (up to 400 ms), we watch the motion of the guest molecule within the cavity. Two processes come to mind: a) a shift of the guest molecule along the longitudinal cavity axis or b) the slow association and dissociation of the molecule including a site exchange of ring 1 and 2.

Further insight into the complex structure was expected by comparing the findings discussed above with the results for the respective *meta*-substituted phenylsulfonate guest (MTS) (Figure 10, 11 and Figure S35a–f). The maximal chemical shift differences of the CD protons induced by complexation with MTS differ by less than 0.06 ppm from those of PTS (see Table 3), indicating a quite similar arrangement of the guest molecule. Using the COSY and ROESY spectra of the complex we could assign all signals to the respective phenyl ring.

Similarly to the complex discussed above, the ROESY spectra of the CD-MTS (1:1) complex show in-phase and out-of-phase correlation peaks. Correlation peaks due to chemical exchange appear between resonances assigned to identical positions on ring 1 (inside) and ring 2 (outside): the triplets at 7.30/7.42 ppm, the doublets at 7.01/7.04 ppm and 6.35/6.57 ppm as well as the singlets at 6.91/6.83 ppm. As in the case of PTS, these spectra strongly point to a slow site exchange in the time range of milliseconds.

Due to the inequivalence of the phenyl protons in MTS, the ROESY spectra were expected to provide more constraints for the placement of the guest molecule within the cavity. For this purpose, we analysed the relevant spectral range displayed in Figure 11.

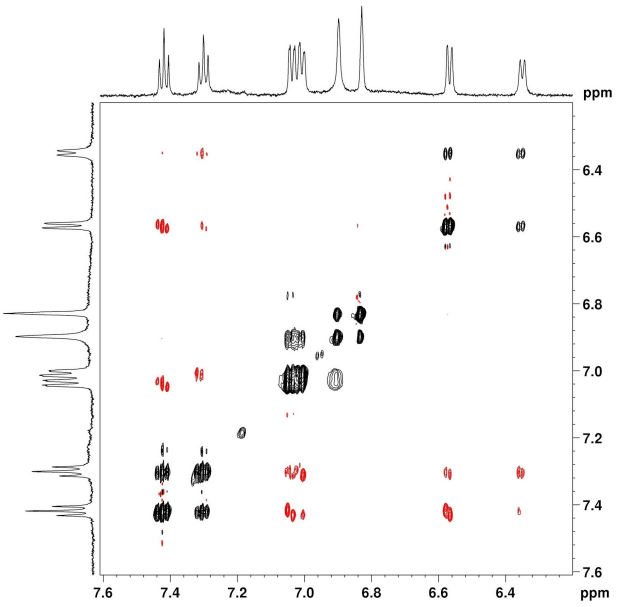

Figure 10. Expansion of the ^{1}H ROESY spectrum for a equimolar aqueous solution of γ-CD with MTS with intense correlations (black) between ring 1 and ring 2 protons and NOE peaks of comparably low intensity (red).

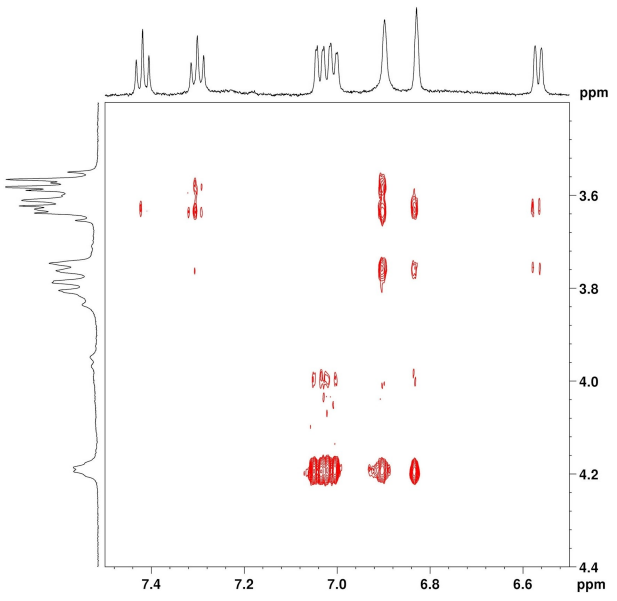

Figure 11. Expansion of the ^{1}H ROESY spectrum for a equimolar aqueous solution of γ-CD with MTS illustrating the NOE between ring 1 and 2 protons as well as methylene protons (4.2 ppm) and cyclodextrin protons.

A strong NOE between the methylene protons and the doublet and singlet signals of both ring protons (7.01/7.04 ppm, 6.91/6.83 ppm) appears evident. The proton at 3.75 ppm assigned to the H5 of cyclodextrin shows distinct correlations to singlet at 6.91 ppm and the doublet signal at 6.35 ppm, which are both signals from protons of ring 1. The correlations to ring 2 signals are significantly weaker. In order to locate ring 1 inside the cavity, the correlation to the H3 signal would be a key information. Unfortunately, the overlap with the resonance of H6a hampers a clear identification of the NOE peaks from protons of ring 1 and ring 2. Furthermore, we notice two correlation peaks between ring 1 singlet and triplet signal and the resonance of H2 and/or H4 having a quite similar chemical shift. Although some of the results are subject to uncertainty, ring 1 can be placed inside the cavity and short distances to the "inner" protons of the cyclodextrin (H3, H5) can be assumed.

The same approach of spectral analysis and peak assignment has been applied to the complexes with the guests PTC and MTC, and the results are qualitatively the same. (See Supporting Information, Figure S36a–f and S37a–f).

As extensively shown, NMR provided a number of valuable information about structure and dynamics of the complexes. Nevertheless, the picture we have so far remains rather qualitative, but the key information – namely, two substituents residing inside the cyclodextrin cavity – was the starting point for in silico investigations. Interestingly, Monte Carlo simulations and docking experiments resulted in complexes where only one of the four arms is located inside the cavity in contrast to our experimental data. We therefore placed the guest molecules manually into the cavity, calculated the binding free energy using MM-GBSA[36] (molecular mechanics generalized Born surface area) and used the resulting structures as starting points for molecular dynamics (MD) simulations. However, if two of the aromatic arms at the central ring are located into the cyclodextrin cavity, these can either be arranged as 1,2-, 1,3- or 1,4-substituents relative to each other (Figure 12). Since we have no experimental evidence that one of the conformations is preferred, complexes with all three possible conformers were considered.

We find that the 1,2 conformations of the four molecules have significantly lower affinities than the 1,3-conformations (~10 kcal/mol); the calculated values are numerically between those of the 1,4-conformations of MTC and PTS in MM-GBSA calculations (Figure S40–S42). The nitrile groups on the central

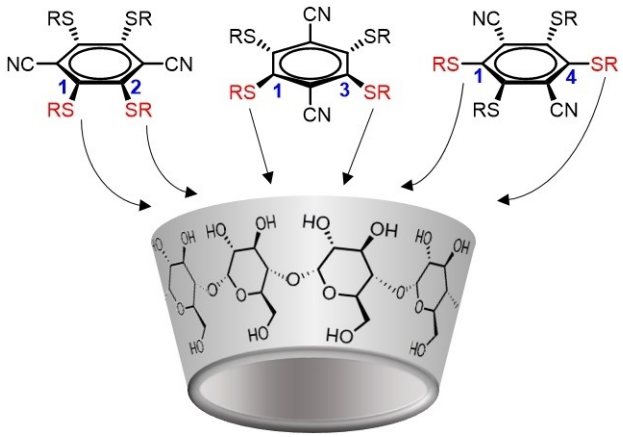

Figure 12. Potential binding modes of the guest compounds with γ-CD featuring two phenyl residues inside (red) and two outside (black) the cavity. The three binding modes are named 1,2, 1,3 and 1,4 indicating the complexed phenyl-rings.

aromatic ring act like an anchor or lid, preventing the entrance of this central element into the cyclodextrin cavity. This can also be seen in MD simulations,[37] where the distance of this central aromatic ring to the centre of γ-cyclodextrin remains at 3–5 Å. (Figure S44, S47, S50, S53). Only the MTS molecule in this particular conformation adopts a position that brings the central ring closer than 2 Å to the cyclodextrin ring. In addition, cyclodextrin must adopt a more elliptical cross section to accommodate the guest in this manner. This binding mode only lasts tens of nanoseconds from 400 ns simulation time onwards.

The 1,3-conformations of the four molecules have the highest affinities in the calculation of the binding energies by the MM-GBSA method (Figure S41). In this binding mode the substituents left and right of the nitrile enter the cavity (Figure 13). This is the only conformation, where the nitrile together with the central aromatic ring can enter the cyclodextrin cavity. This is reflected in the Van der Waals (VdW) contribution to the binding energy (Figure S43). In all other conformations, the nitriles are located outside the cavity like an anchor. In the MD simulations, these complexes show a surprisingly high flexibility. The central ring can be accommodated almost in the centre of the cyclodextrin cavity (1 Å) and it is tilted upward for this purpose, which is reflected in a large angle towards the cyclodextrin ring (Figure S45, S48, S51, S54).

All four molecules are able to establish a close binding within the cavity, but – in accordance to the ROESY experiments – show also a strong tendency to move the central ring to the outside of the cyclodextrin cavity (which is reflected by an increase in the distance between the rings as well as a decrease in the angle between them). In fact, the latter one appears to be the energetically favoured binding mode. Our original hypothesis was that a distinct conformation would discriminate between the luminescent *meta*- and the non-luminescent *para*-molecules. However, this does not appear to be the case. All molecules can accommodate both conformations. But the *meta*-derivatives reside over extended timespans in a state, where the central ring is outside the cyclodextrin ring. This is most prominent for the MTC molecule, which after an initial phase inside the cavity only binds the γ-CD ring outside the cyclodextrin ring. In the case of MTS, a rather fast alternation between the two types of binding is observed. The other two molecules (PTS and PTC) were observed only to short periods of the simulation time binding their central ring to end of the cyclodextrin conus. Therefore, the complexation does not appear to be as rigid or static as one would imagine, but rather defined by a period when the molecule is rigid (i.e., stable angle of the central ring relative to the cyclodextrin as well as a stable angle of the phenyl substituents relative to each other). The distinction from the *para*-substituted molecules PTC and PTS seems to be the stabilization of this binding mode, which could be caused by the possible electrostatic interactions of the charged groups. These are closer together in the *meta*-variants than in the *para*-molecules.

Analogous to the complexes with the 1,2-conformation, the 1,4 conformation of the molecules have lower affinities than the 1,3-conformations (1–15 kcal/mol; Figure S42). Again, the nitrile groups on the central aromatic ring act like an anchor, preventing the entrance of this central element into the cyclodextrin cavity. This can be seen by longer distances between this central aromatic ring and the centre of γ-cyclodextrin (3–6 Å; Figure S46, S49, S52, S55).

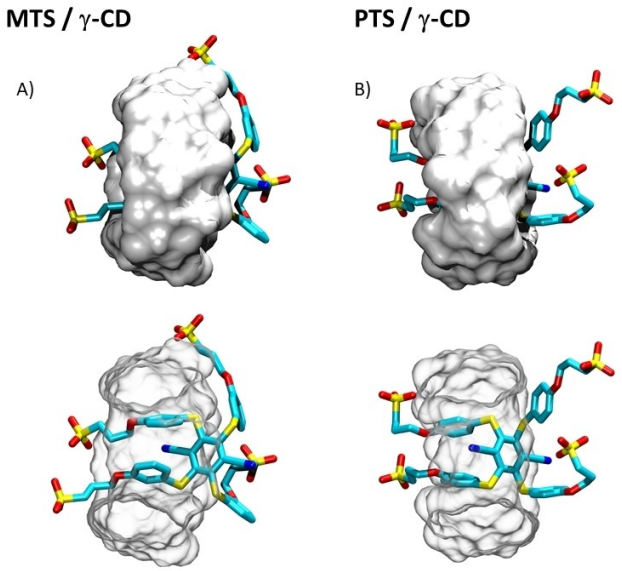

Figure 13. Representative conformations from molecular dynamics simulations of A) MTS and B) PTS as a 1:1 complex with γ-CD.

Conclusion

We reported the first examples of water soluble RTP compounds involving γ-CD host-guest systems. The calorimetric data show an outstanding association constant for organic dyes (K_a values from 1.52×10^5 M^{-1} to 5.13×10^5 M^{-1}), comparable only with strongly binding compounds, such as organic nanodiamonds[29] and inorganic borate clusters.[30] The cage formation investigated by NMR and theoretical simulation reduces the rotational and vibrational quenching modes, and it is able to protect the aromatic guest from interaction with oxygen, similar to the behaviour of naphthalene in β-CD,[23] resulting in a "switch on" of the phosphorescence emission. However, this effect is strictly connected with regioisomeric configuration of the dyes, emphasizing the pivotal role of the molecular design to realize new water-soluble RTP systems. Indeed, the host-guest complexes with para-substituents are showing higher binding constants (4.99 and 5.13×10^5 M^{-1} for PTS and PTC, respectively) but no "RTP switch on" behaviour, whereas the meta-substituted dyes have slightly lower K_a values (1.53 and 1.52×10^5 M^{-1} for MTS and MTC, respectively) and RTP character. The reported innovative metal-free RTP systems in aqueous solution open novel scenarios for application in bioimaging, optical sensors and many other fields, by means of their possible use as indicators in displacement assays. Besides that, the finding that a high association constant does not necessarily lead to an emission "on"

behaviour, is a very important lesson learned and will have an impact on upcoming studies, involving the design and application of RTP active biomedical ligands.

Acknowledgements

J.V. and M.H. acknowledges the CRC 1093 (project number: 229838028, project A10) for financial support. F.R. thanks DFG (grant n. RI 2635/6-1, project number: 464509280) and Westfälische Wilhelms-Universität Münster for financial support. G.H.C. thanks the Deutsche Forschungsgemeinschaft (GRK2376 "Confinement-controlled Chemistry" – project number 331085229). Laura Schneider is acknowledged for the mass spectrometric measurements of the inclusion complexes. We furthermore thank Sven Kather and Alyssia Daniels for support during the measurements. Additionally we thank Dr. Christine Beuck and M. Sc. Alexander Huber for fruitful discussions. Open Access funding enabled and organized by Projekt DEAL.

Conflict of Interest

The authors declare no conflict of interest.

Data Availability Statement

The data that support the findings of this study are available from the corresponding author upon reasonable request.

Keywords: cyclodextrins · host-guest systems · isothermal titration calorimetry · room temperature phosphorescence · supramolecular chemistry

[1] a) Y. He, N. H. Cheng, X. Xu, J. W. Fu, J. A. Wang, *Org. Electron.* **2019**, *64*, 247–251; b) H. F. Higginbotham, M. Okazaki, P. de Silva, S. Minakata, Y. Takeda, P. Data, *ACS Appl. Mater. Interfaces* **2021**, *13*, 2899–2907.

[2] a) J. H. Yum, B. E. Hardin, S. J. Moon, E. Baranoff, F. Nuesch, M. D. McGehee, M. Grätzel, M. K. Nazeeruddin, *Angew. Chem. Int. Ed.* **2009**, *48*, 9277–9280; *Angew. Chem.* **2009**, *121*, 9441–9444; b) A. B. Alemayehu, N. U. Day, T. Mani, A. B. Rudine, K. E. Thomas, O. A. Gederaas, S. A. Vinogradov, C. C. Wamser, A. Ghosh, *ACS Appl. Mater. Interfaces* **2016**, *8*, 18935–18942; c) W. L. Zhou, Y. Chen, Q. Yu, H. Zhang, Z. X. Liu, X. Y. Dai, J. J. Li, Y. Liu, *Nat. Commun.* **2020**, *11*, 4655.

[3] a) H. Braunschweig, T. Dellermann, R. D. Dewhurst, B. Hupp, T. Kramer, J. D. Mattock, J. Mies, A. K. Phukan, A. Steffen, A. Vargas, *J. Am. Chem. Soc.* **2017**, *139*, 4887–4893; b) V. Sathish, A. Ramdass, P. Thanasekaran, K. L. Lu, S. Rajagopal, *J. Photochem. Photobiol. C* **2015**, *23*, 25–44; c) E. Holder, B. M. W. Langeveld U S Schubert, *Adv. Mater.* **2005**, *17*, 1109–1121.

[4] a) M. Hayduk, S. Riebe, J. Voskuhl, *Chem. Eur. J.* **2018**, *24*, 12221–12230; b) S. Mukherjee, P. Thilagar, *Chem. Commun.* **2015**, *51*, 10988–11003; c) B. Roy, I. Maisuls, J. Zhang, F. C. Niemeyer, F. Rizzo, C. Wolper, C. G. Daniliuc, B. Z. Tang, C. A. Strassert, J. Voskuhl, *Angew. Chem. Int. Ed.* **2022**, *61*, e202111805; *Angew. Chem.* **2022**, *134*, e202111805.

[5] S. Hirata, *Adv. Opt. Mater.* **2017**, *5*, 1700116.

[6] a) D. Lee, O. Bolton, B. C. Kim, J. H. Youk, S. Takayama, J. Kim, *J. Am. Chem. Soc.* **2013**, *135*, 6325–6329; b) D. Li, Y. Yang, J. Yang, M. Fang, B. Z. Tang, Z. Li, *Nat. Commun.* **2022**, *13*, 347.

[7] a) C. Chen, R. Huang, A. S. Batsanov, P. Pander, Y. T. Hsu, Z. Chi, F. B. Dias, M. R. Bryce, *Angew. Chem. Int. Ed.* **2018**, *57*, 16407–16411; *Angew. Chem.* **2018**, *130*, 16645–16649; b) C. A. M. Salla, G. Farias, M. Rouzieres, P. Dechambenoit, F. Durola, H. Bock, B. de Souza, I. H. Bechtold, *Angew. Chem. Int. Ed.* **2019**, *58*, 6982–6986; *Angew. Chem.* **2019**, *131*, 7056–7060; c) Y. Xiong, Z. Zhao, W. Zhao, H. Ma, Q. Peng, Z. He, X. Zhang, Y. Chen, X. He, J. W. Y. Lam, B. Z. Tang, *Angew. Chem. Int. Ed.* **2018**, *57*, 7997–8001; *Angew. Chem.* **2018**, *130*, 8129–8133.

[8] L. Xiao, H. Fu, *Chem. Eur. J.* **2019**, *25*, 714–723.

[9] L. Gu, H. F. Shi, L. F. Bian, M. X. Gu, K. Ling, X. Wang, H. L. Ma, S. Z. Cai, W. H. Ning, L. S. Fu, H. Wang, S. Wang, Y. R. Gao, W. Yao, F. W. Huo, Y. T. Tao, Z. F. An, X. G. Liu, W. Huang, *Nat. Photonics* **2019**, *13*, 406–411.

[10] a) S. Guo, W. B. Dai, X. A. Chen, Y. X. Lei, J. B. Shi, B. Tong, Z. X. Cai, Y. P. Dong, *ACS Materials Lett.* **2021**, *3*, 379–397; b) X. K. Ma, Y. Liu, *Acc. Chem. Res.* **2021**, *54*, 3403–3414; c) G. Qu, Y. Zhang, X. Ma, *Chin. Chem. Lett.* **2019**, *30*, 1809–1814; d) S. Horiuchi, C. Matsuo, E. Sakuda, Y. Arikawa, G. H. Clever, K. Umakoshi, *Dalton Trans.* **2020**, *49*, 8472–8477.

[11] J. Wang, Z. Huang, X. Ma, H. Tian, *Angew. Chem. Int. Ed.* **2020**, *59*, 9928–9933; *Angew. Chem.* **2020**, *132*, 10014–10019.

[12] a) K. Kim, N. Selvapalam, Y. H. Ko, K. M. Park, D. Kim, J. Kim, *Chem. Soc. Rev.* **2007**, *36*, 267–279; b) R. S. Cicolani, L. R. R. Souza, G. B. de Santana Dias, J. M. R. Gonçalves, I. d S Abrahão, V. M. Silva, G. J.-F. Demets, *J. Inclusion Phenom. Macrocyclic Chem.* **2020**, *99*, 1–12; c) D. Das, K. I. Assaf, W. M. Nau, *Front. Chem.* **2019**, *7*, 619.

[13] a) D. Kauerhof, J. Niemeyer, *ChemPlusChem* **2020**, *85*, 889–899; b) G. Crini, *Chem. Rev.* **2014**, *114*, 10940–10975.

[14] a) A. Cid-Samamed, J. Rakmai, J. C. Mejuto, J. Simal-Gandara, G. Astray, *Food Chem.* **2022**, *384*, 132467; b) M. Q. Zhang, D. C. Rees, *Expert Opin. Ther. Pat.* **1999**, *9*, 1697–1717; c) H.-Y. Chen, M. Zhao, J.-H. Tan, Z.-S. Huang, G.-F. Liu, L.-N. Ji, Z.-W. Mao, *Tetrahedron* **2014**, *70*, 2378–2382.

[15] a) A. Khalid, Asim-ur-Rehman, N. Ahmed, I. Chaudhery, M. A. Al-Jafary, E. A. Al-Suhaimi, M. Tarhini, N. Lebaz, A. Elaissari, *Chem. Eur. J.* **2021**, *27*, 8437–8451; b) M. Cacciarini, M. B. Nielsen, E. M. de Castro, L. Marinescu, M. Bols, *Tetrahedron Lett.* **2012**, *53*, 973–976, https://chemistry-europe.onlinelibrary.wiley.com/action/showCitFormats?doi=10.1002%2Fchem.202100204.

[16] a) Y. C. Chen, J. W. Y. Lam, R. T. K. Kwok, B. Liu, B. Z. Tang, *Mater. Horiz.* **2019**, *6*, 428–433; b) Z. Zhao, H. Zhang, J. W. Y. Lam, B. Z. Tang, *Angew. Chem. Int. Ed.* **2020**, *59*, 9888–9907; *Angew. Chem.* **2020**, *132*, 9972–9993; c) F. Würthner, *Angew. Chem. Int. Ed.* **2020**, *59*, 14192–14196; *Angew. Chem.* **2020**, *132*, 14296–14301.

[17] a) S. Xie, A. Y. H. Wong, S. Chen, B. Z. Tang, *Chem. Eur. J.* **2019**, *25*, 5824–5847; b) H. T. Feng, J. W. Y. Lam, B. Z. Tang, *Coord. Chem. Rev.* **2020**, *406*, 213142; c) Y. Huang, J. Ji, J. Zhang, F. Wang, J. Lei, *Chem. Commun.* **2019**, *56*, 313–316.

[18] N. L. Leung, N. Xie, W. Yuan, Y. Liu, Q. Wu, Q. Peng, Q. Miao, J. W. Lam, B. Z. Tang, *Chem. Eur. J.* **2014**, *20*, 15349–15353.

[19] Y. Liu, A. Qin, X. Chen, X. Y. Shen, L. Tong, R. Hu, J. Z. Sun, B. Z. Tang, *Chem. Eur. J.* **2011**, *17*, 14736–14740.

[20] S. Song, H. F. Zheng, D. M. Li, J. H. Wang, H. T. Feng, Z. H. Zhu, Y. C. Chen, Y. S. Zheng, *Org. Lett.* **2014**, *16*, 2170–2173.

[21] Y. Gao, B. Han, Y. T. Chen, X. Wang, M. Bai, *RSC Adv.* **2016**, *6*, 16581–16585.

[22] a) Y. Zhang, D. Yang, J. Han, J. Zhou, Q. Jin, M. Liu, P. Duan, *Langmuir* **2018**, *34*, 5821–5830; b) M. Levine, B. R. Smith, *J. Fluoresc.* **2020**, *30*, 1015–1023.

[23] V. Avakyan, V. Nazarov, M. V. Alfimov, *Naphthalene. Structure, Properties and Applications* (Eds.: G. I. Antsyforov, A. F. Ivanski), Nova Scinence Publishers, Inc. New York **2012**, pp. 127–152.

[24] a) S. Riebe, C. Wölper, J. Balszuweit, M. Hayduk, M. E. Gutierrez Suburu, C. A. Strassert, N. L. Doltsinis, J. Voskuhl, *ChemPhotoChem* **2020**, *4*, 384–384; b) S. Riebe, C. Vallet, F. van der Vight, D. Gonzalez-Abradelo, C. Wölper, C. A. Strassert, G. Jansen, S. Knauer, J. Voskuhl, *Chem. Eur. J.* **2017**, *23*, 13660–13668.

[25] W. Xi, J. Yu, M. Wei, Q. Qiu, P. Xu, Z. Qian, H. Feng, *Chem. Eur. J.* **2020**, *26*, 3733–3737.

[26] M. Hayduk, S. Riebe, K. Rudolph, S. Schwarze, F. van der Vight, C. G. Daniliuc, G. Jansen, J. Voskuhl, *Isr. J. Chem.* **2018**, *58*, 927–931.

[27] P. Ahlers, C. Gotz, S. Riebe, M. Zirbes, M. Jochem, D. Spitzer, J. Voskuhl, T. Basche, P. Besenius, *Polym. Chem.* **2019**, *10*, 3163–3169.

[28] J. Mei, N. L. Leung, R. T. Kwok, J. W. Lam, B. Z. Tang, *Chem. Rev.* **2015**, *115*, 11718–11940.

[29] a) J. Voskuhl, M. Waller, S. Bandaru, B. A. Tkachenko, C. Fregonese, B. Wibbeling, P. R. Schreiner, B. J. Ravoo, *Org. Biomol. Chem.* **2012**, *10*, 4524–4530; b) F. Schibilla, J. Voskuhl, N. A. Fokina, J. E. P. Dahl, P. R. Schreiner, B. J. Ravoo, *Chem. Eur. J.* **2017**, *23*, 16059–16065.

[30] a) K. I. Assaf, M. S. Ural, F. Pan, T. Georgiev, S. Simova, K. Rissanen, D. Gabel, W. M. Nau, *Angew. Chem. Int. Ed.* **2015**, *54*, 6852–6856; *Angew.*

Chem. **2015**, *127*, 6956–6960; b) K. I. Assaf, D. Gabel, W. Zimmermann, W. M. Nau, *Org. Biomol. Chem.* **2016**, *14*, 7702–7706; c) J. Nekvinda, B. Gruner, D. Gabel, W. M. Nau, K. I. Assaf, *Chem. Eur. J.* **2018**, *24*, 12970–12975.
[31] M. V. Rekharsky, Y. Inoue, *Chem. Rev.* **1998**, *98*, 1875–1918.
[32] a) M. Baroncini, G. Bergamini, P. Ceroni, *Chem. Commun.* **2017**, *53*, 2081–2093; b) A. Fermi, G. Bergamini, M. Roy, M. Gingras, P. Ceroni, *J. Am. Chem. Soc.* **2014**, *136*, 6395–6400.
[33] C. J. Easley, M. Mettry, E. M. Moses, R. J. Hooley, C. J. Bardeen, *J. Phys. Chem. A* **2018**, *122*, 6578–6584.
[34] K. A. Connors, *Chem. Rev.* **1997**, *97*, 1325–1358.
[35] H. J. Schneider, F. Hacket, V. Rudiger, H. Ikeda, *Chem. Rev.* **1998**, *98*, 1755–1786.
[36] P. A. Kollman, I. Massova, C. Reyes, B. Kuhn, S. Huo, L. Chong, M. Lee, T. Lee, Y. Duan, W. Wang, O. Donini, P. Cieplak, J. Srinivasan, D. A. Case, T. E. Cheatham, *Acc. Chem. Res.* **2000**, *33*, 889–897.
[37] K. J. Bowers, D. E. Chow, H. Xu, R. O. Dror, M. P. Eastwood, B. A. Gregersen, J. L. Klepeis, I. Kolossvary, M. A. Moraes, F. D. Sacerdoti, J. K. Salmon, Y. Shan, D. E. Shaw, *SC '06: Proceedings of the 2006 ACM/IEEE Conference on Supercomputing* **2006**, pp. 43–43, doi: 10.1109/SC.2006.54.

Manuscript received: April 8, 2022
Accepted manuscript online: June 13, 2022
Version of record online: July 25, 2022